PETROLOGY, DIAGENESIS AND RESERVOIR QUALITY OF CORE SAMPLES FROM YOLLA-2, T-RL-1, BASS BASIN

by

K. R. Martin MSc, PhD

A report to :

Geotechnical Services Pty Ltd
41-45 Furnace Road
WELSHPOOL,   WA   6106

28th January, 1999

K.R. MARTIN PTY LTD ACN 010 141 107 PO BOX 22 KENMORE QUEENSLAND AUSTRALIA 4069

C O N T E N T S

FIGURES AND TABLES

1. INTRODUCTION

Yolla-2, located in T-RL-1, Bass Basin, was spudded on 9th April,1998 and was plugged and abandoned after reaching a total depth of 3165m on 25th June, 1998.

Fifteen samples, mostly horizontal plug offcuts, were provided for petrological analysis. Table 1 lists the petrological analyses carried out on each sample, as well as results of routine core analysis carried out by Geotechnical Services Pty Ltd.

TABLE 1. SAMPLE DEPTHS AND ANALYSES PERFORMED

			PETROLOGICAL ANALYSIS				CORE ANALYSIS	
Plug	Depth (m)	Samp Type	TSA	XRD	SEM	PM	Porosity (%)	Perm. (mD)
1	3033.03	Plug end	x			x	14.1	7.5
-	3034.05	Vert plug	x	x	x	x	16.8	14
8	3035.15	Plug end	x				9.2	<0.1
14	3036.95	Plug end	x		x	x	18.3	208
17	3037.84	Plug end	x	x			10.7	0.26
21	3039.06	Plug end	x				5.4	<0.1
27	3040.81	Plug end	x			x	30.7	1678
30	3041.70	Plug end	x	x			23.2	4726
35	3043.21	Plug end	x				24.5	>10000
-	3045.00	Core chip	x	x			18.2	503
45	3046.14	Plug end	x	x			13.8	6.1
50	3047.67	Plug end	x				18.2	674
52	3048.19	Plug end	x		x		16.2	319
56	3049.44	Plug end	x	x			4.3	<0.1
59	3050.17	Plug end	x				13.0	0.36

TSA=thin-section analysis XRD=X-ray diffraction analysis SEM=scanning electron microscopy PM=photomicoscopy

1. ANALYTICAL PROGRAM

1.1 THIN-SECTION ANALYSIS

All samples were impregnated with blue dyed epoxy resin and thin-sections were prepared by cutting and grinding in kerosene to minimise any potential for sample damage due to freshwater sensitivity. Rock composition and visible porosity were determined by a count of 350 points in each thin-section. No systematic grain size analysis was carried out, but the average grain size and sorting were estimated in thin-section with the aid of an eyepiece graticule.

Photomicrographs were taken of a selection of samples to illustrate features described from thin-section.

1.2 X-RAY DIFFRACTION ANALYSIS

Qualitative XRD analysis of the fine fraction from six samples was carried out to identify their clay mineralogy. A portion of each sample was disaggregated in distilled water and the fine suspended fraction was air-dried on glass discs to produce orientated specimens for analysis. This technique concentrates the clay minerals, and orientation enhances the main clay mineral reflections allowing positive identification even when clay minerals are present in only low concentrations. Each sample was analysed in air-dried condition and also after treatment with ethylene glycol to detect the presence of any swelling clays. X-ray traces for the six samples are presented in Appendix 1.

1.3 SCANNING ELECTRON MICROSCOPY

Three samples were examined with the SEM to provide additional information about porosity distribution and origin, as well the morphology and distribution of clays and cements throughout the pore system.

3. TEXTURE

Estimates of average grain size and sorting are given in Table 2. There is a large variation in grain size within the sample suite, with a size range from 0.03mm (medium-coarse silt) to 3.0mm (granule conglomerate). Thirteen of the 15 samples have average grain sizes in the fine sand to very coarse sand range. The most fine-grained samples contain obvious laminations but the coarser grained sands appear more homogeneous except where the presence of micaceous laminae or carbonaceous fragments define layering in a few samples (e.g. Plug 17, 3037.84m)

Most samples are moderately well sorted and although there is some variation in sorting, it appears unrelated to grain size.

TABLE 2. THIN-SECTION ANALYSIS

Sample	Depth (m)	GSmm	Sorting	Qzm	Qzc	Cht	Fel	Irf	Mrf	Srf	Mic	HM	Opq	Sid	Ank	Clay	Vpor
1	3033.03	0.30	mw	65.6	6.9	1.1		0.3	1.4	0.6	1.4		1.4			13.3	8.1
	3034.05	0.35	mw	58.6	5.7	0.9		0.3	3.1	1.1	0.3			7.4	0.3	12.6	9.7
8	3035.15	0.24	mw	58.0	4.9	0.9		0.9	2.0	1.4	2.0		1.7	5.7	0.3	20.0	2.3
14	3036.95	0.30	w	71.1	5.1	0.6			0.9	0.9				0.6	1.4	6.9	12.6
17	3037.84	0.28	m	53.4	7.4	2.0		0.3	3.4	1.4	4.9	0.3	2.9	0.3	0.3	21.4	2.0
21	3039.06	0.03	mw	45.4							10.0	1.1	2.9	6.3		34.3	0.0
27	3040.81	1.25	mw	67.1	10.9	1.1			0.3	0.3						5.1	15.1
30	3041.70	1.25	mw	64.8	12.7	1.0			1.3	0.3						3.8	16.2
35	3043.21	1.20	mw	64.9	7.7	0.3		0.3	2.9	0.6						4.3	19.1
	3045.00	3.00	mw	29.7	36.0	10.6			9.4	0.3	0.3		0.3			3.1	10.3
45	3046.14	0.30	m	63.1	8.7	1.4		0.3	3.1		0.8		0.3	2.3		15.2	4.8
50	3047.67	0.90	p	62.6	17.4	2.0			1.4							6.0	10.6
52	3048.19	0.50	mw	77.1	6.0	0.9			0.3	1.1						5.7	8.9
56	3049.44	0.13	mw	34.4	6.5	0.9	0.3	1.1	6.5	2.3	4.3	0.3	4.8	6.8		31.8	0.0
59	3050.17	0.22	w	49.7	5.7	0.9	0.3		2.0	0.3	0.9		1.7	16.0	0.9	19.4	2.3

Qzm=monocrystalline quartz Qzc=composite quartz Cht=chert Fel=feldspar Irf=igneous rock fragments Mrf=metamorphic rock fragments Srf=sedimentary rock fragments Mic=mica HM=heavy minerals Opq=opaques Sid=siderite Ank=ankerite Vpor=visible porosity

4. COMPOSITION

Results of thin-section point count analysis are presented in Table 2, the recalculated QFR ratios are given in Table 3 and the QFR data are plotted on a ternary sandstone compositional diagram (Figure 1).

In their detrital grain composition, the majority of the sandstones may be classified as quartzarenites, having QFR compositions with more than 95% quartz + chert. The remainder are sublitharenites which contain somewhat lower quartz content and instead they contain significant lithic grains.

During point count analysis, monocrystalline and polycrystalline (composite) quartz grains were separated (Table 2.). In all but one of the samples, monocrystalline quartz is considerably more abundant than polycrystalline quartz, although in several samples polycrystalline quartz constituted more than 10% of the rock. At 3045.00m, which is the most coarse grained sample in the suite, polycrystalline quartz (36.0%) is more abundant than monocrystalline quartz (29.7%). In addition, this sample contains 10.6% chert, which does not exceed 2% in any other sample. The increase in composite quartz, most of which appears to be of metamorphic origin, is related mainly to increasing grain size. It is a predictable relationship, with coarser grain sizes more likely to include composite grains and rock fragments than the finer grain sizes, where the average grain size of the sand is more likely to be below the average grain size of individual crystals making up the composite grains.

Feldspar is almost totally absent from the interval and only in the two deepest samples were isolated grains of feldspar recorded in the analyses. The absence of feldspar is likely to be due to its decomposition to authigenic clay.

Lithic grains were recorded in all samples except the siltstone (Plug 21, 3039.06m) in amounts up to 9.9%. The most abundant lithic types are low-grade regional metamorphic rocks (quartz-mica schist and phyllite) and there are also smaller numbers of sedimentary rock fragments (shale, siltstone) and rare altered acid volcanic rock fragments.

TABLE 3. QFR RATIOS

Plug Number	Depth (m)	**Q** Quartz+Chert	**F** Feldspar	**R** Rock Fragments
1	3033.03	97.0	0.0	3.0
-	3034.05	93.5	0.0	6.5
8	3035.15	93.7	0.0	6.3
14	3036.95	97.7	0.0	2.3
17	3037.84	92.5	0.0	7.5
21	3039.06	100.0	0.0	0.0
27	3040.81	99.2	0.0	0.8
30	3041.70	98.0	0.0	2.0
35	3043.21	95.0	0.0	5.0
-	3045.00	88.7	0.0	11.3
45	3046.14	95.6	0.0	4.4
50	3047.67	98.3	0.0	1.7
52	3048.19	98.4	0.0	1.6
56	3049.44	80.4	0.6	19.0
59	3050.17	95.6	0.5	3.9

FIGURE 1. QFR COMPOSITIONS

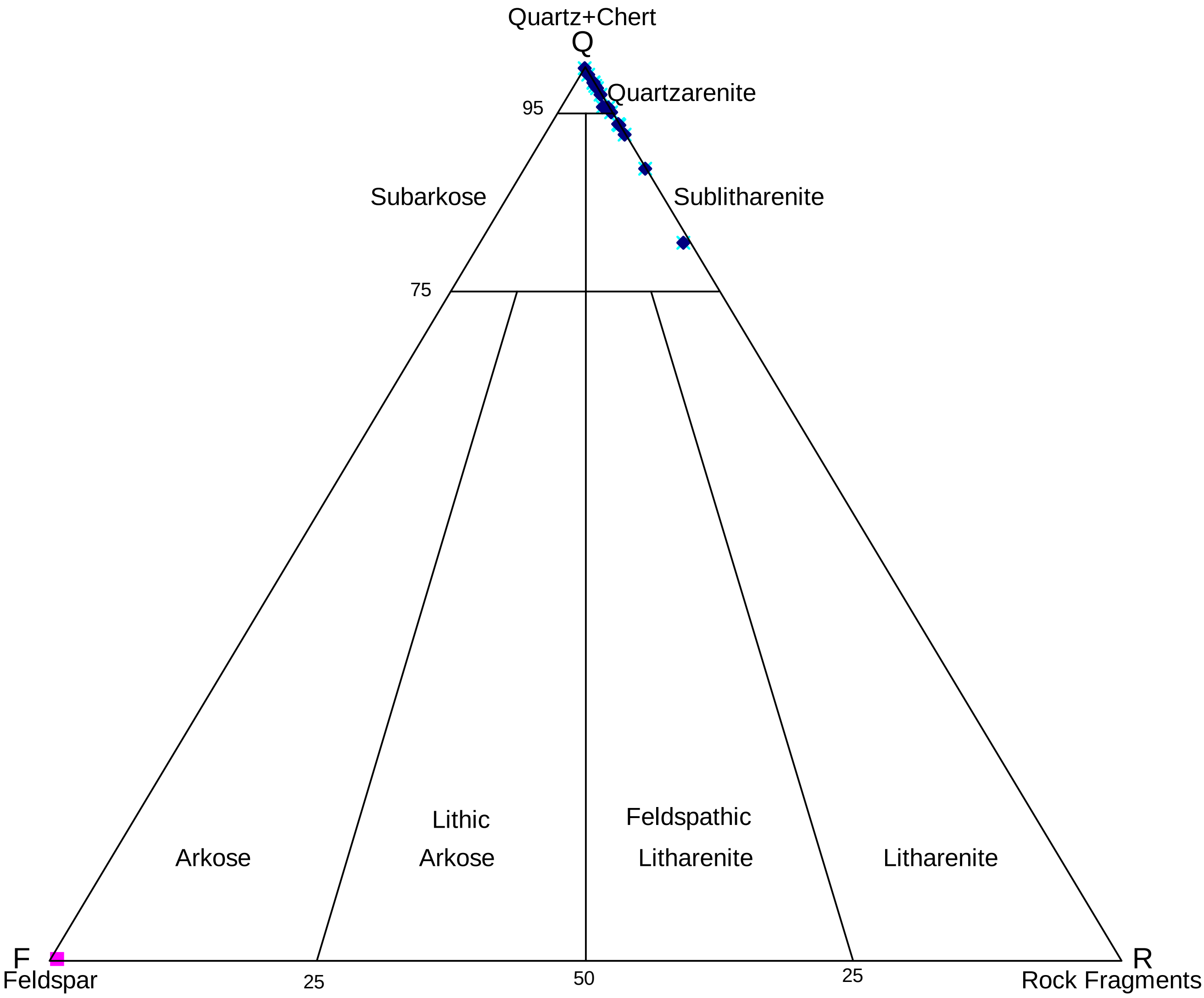

Mica is rare in the coarser grained sands but is an important component of some of the finer grained samples where it occurs in amounts between 2.0 and 10.0%. However, the original mica content of many of the samples may have been considerably higher, as there is evidence of widespread decomposition of mica and micaceous rock fragments to authigenic clay, as well as their replacement by authigenic siderite.

Opaques are concentrated mainly within the finer grained samples and they were not recorded in most of the coarse-very coarse samples. Opaques consist mainly of carbonaceous material and less commonly of leucoxene. Pyrite is rare and was recorded as a local replacement of carbonaceous material in Plug 17, 3037.84m only.

Carbonate was recorded in eight of the samples but it is important (>5%) in only five sample. The carbonate is mostly fine grained siderite except at 3036.95m where more coarsely crystalline ankerite is sporadically distributed through the pore system and may represent remnants of a previously more widespread cement. Fine grained siderite cement is most abundant at 3050.17m where it makes up 16.0% of the rock. It occurs in a similar form at 3034.05m whereas at 3035.15m, 3039.06m and 3044.44m siderite is more erratic in its distribution and it occurs mainly as a replacement of labile grains, particularly biotite mica.

Clay content ranges from 3.1% to 34.3% and averages 13.5% in the 15 samples. Clay increases with decreasing grain size, and all sands above medium sand contain less than 10% clay whereas samples below medium sand typically contain at least 20% clay. Almost all the clay in the Yolla-2 sandstones appears to be authigenic. Kaolin clays (kaolinite, dickite) dominate in the medium and coarse grained sands and occur as loosely packed pore fillings and as large grain-sized patches where labile grains (probably mostly feldspar) have totally decomposed. In the finer grained samples, authigenic illite and/or illite/smectite assume greater importance, because of the abundance of mica and micaceous rock fragment precursors.

The clay mineralogy of the Yolla-2 samples was determined by qualitative XRD analysis of six samples. Results are given in Table 4 and show that kaolin clays are either dominant or abundant in all samples, with dickite occurring in four of the samples and kaolinite in only two. Illite, which may include some fine grained mica, occurs consistently as a minor

TABLE 4. X-RAY DIFFRACTION ANALYSIS

Plug No	Depth (m)	Kaolinite	Dickite	Illite	Illite/smec	Quartz	Siderite
-	3034.05	-	A	M	T	A	M
17	3037.84	A	-	M	M	A	-
30	3041.70	-	D	M	-	M	-
-	3045.00	-	A	M	-	A	-
45	3046.14	-	D	M	-	M	-
56	3049.44	A	-	M	A	M	M

D=dominant A=abundant M=minor T=trace (estimated relative abundance in clay fraction)

component in all samples. Illite/smectite was recorded in three samples. It is an abundant constituent of Plug 56, 3049.44m, which is the most fine grained sample analysed. The illite/smectite mixed layer clay is an ordered (regularly interstratified) illite-rich variety with a smectite content of <15% (Appendix 1).

Visible macroporosity in thin-section generally increases with increasing grain size and reaches a maximum of 19.1%. The two most fine grained samples lack visible porosity. Most porosity appears to be intergranular, but the presence of oversized pores in some sands as well as corroded ankerite crystals within the pore system of some samples suggests that some secondary pores may have formed due to either labile grain or carbonate cement dissolution.

5. DIAGENESIS

Diagenetic processes exert a major influence on reservoir quality. The most important processes are cementation by quartz overgrowths and the formation of authigenic clays. Locally important but less widespread processes are carbonate cementation/replacement and grain contact dissolution. Compaction-induced deformation of ductile framework grains such as micaceous rock fragments is significant as a cause of porosity loss only in those few samples where ductile grain content (lithics, mica) is relatively elevated (e.g. Plug 56, 3049.44m). However, it is often difficult to distinguish between purely compactional effects and those due to grain contact dissolution (pressure solution) or deformation/dispersion of labile grains associated with the onset of decomposition to authigenic clays.

Quartz overgrowth cementation appears most advanced in some of the cleaner medium grained sands (e.g. Plug 14, 3036.95m) where overgrowths are an important cause of porosity reduction (Plate 5, Figure 1) and may in places totally occlude some intergranular pores. In the finer grained samples, overgrowth development has often been inhibited to varying degrees by the presence of earlier-formed authigenic clay and carbonates which occupy much of the pore system. In the most coarse grained sample (3045.99m), overgrowths appear to be less advanced than in some of the medium grained sands, possibly due to the greater prevalence of composite quartz grains which often show little overgrowth development.

Authigenic clay is present in all samples and is a product of the decomposition of labile framework grains including mica, lithics and almost certainly feldspar. The almost total lack of feldspar through the interval, together with the common presence of kaolin pore fillings particularly as large grain-sized patches (Plate 1, Figure 1), strongly suggests that the main precursor of kaolin clays (both dickite and kaolinite) is likely to have been feldspar. In addition, at least some of the mica and micaceous rock fragments appears to be decomposing to kaolin, although illite and illite/smectite are the more usual alteration products of mica and lithics (Plate 4, Figure 1).

The presence of dickite instead of kaolinite in most of the samples analysed by XRD is likely to be due to replacement of kaolinite in response to increasing burial depth and temperature. The occurrence of dickite in sandstone reservoirs has been reviewed by Ehrenberg et al (1993) who concluded that the transformation from kaolinite probably took place at temperatures of around 120^{o}C. They also noted that the transformation occurred most readily in higher permeability sandstones. These conclusions are in agreement with the author’s own observations in several Australian basins where dickite is characteristic of deeply buried, high-temperature reservoirs. In these dickite-bearing reservoirs, any remaining kaolinite is usually present only in low permeability sandstones. This is the case in Yolla-2 where the two samples containing kaolinite both have permeability well below 1mD.

In the finer grained samples from Yolla-2, illitic clays (illite, illite/smectite) assume greater importance because they are common alteration products of mica and micaceous rock fragments which are more concentrated in the finer grained sands (Plate 3, Figure 2). Although illitic clays appear to precede dickite and quartz overgrowths, their timing with respect to kaolinite remains uncertain.

The formation of authigenic siderite was one of the earliest diagenetic changes to take place. The siderite lines and fills pores and also replaces some labile grains, particularly mica and lithics. It has been encapsulated by later quartz overgrowths and it surrounds large pores in which grains have altered to kaolinite, which it also precedes. Siderite precedes ankerite, although the timing of ankerite formation, particularly with respect to kaolinite, is difficult to establish. Ankerite is tentatively suggested to post-date kaolinite, with later dissolution and corrosion of the carbonate occurring prior to, or coeval quartz overgrowth formation.

Grain contact dissolution (pressure solution) is an important process in those samples where quartz overgrowth formation has been restricted. This occurs mostly in finer grained samples (eg. Plug 56, 3049.44m) or within finer grained laminae where clay and decomposing mica are concentrated. The process causes tighter grain packing and porosity loss, as dissolution at grain contacts leads to elongate, undulose and sutured grain contacts, and sometimes results the formation of zones of microstylolites which traverse the full width of the thin-section. Grain contact dissolution is also common in the most coarse grained sample (3045.00m) where quartz overgrowths are rare, probably because of the high incidence of composite quartz and chert. Grain contact dissolution probably precedes quartz overgrowth formation and may accompany or closely follow the decomposition of mica and rock fragments to illitic clays.

Although decomposition of labile grains has produced mainly clay-filled pores, there also appears to have been some dissolution of labile grains and possibly ankerite cement to form secondary porosity. Oversized pores are relatively common in many of the medium-very coarse grained samples and some contain corroded ankerite crystals while others are partly filled by authigenic clay and remnants of the decomposed/dissolved grains. Secondary porosity formation probably took place mostly before quartz overgrowth cementation but some secondary porosity formation may have continued after cessation of overgrowth cementation.

The suggested paragenetic sequence for the Yolla-2 sandstones is shown diagrammatically in Figure 2.

Authigenic Siderite	xxxxxxx
Authigenic Kaolinite	xxxxxxxxxx
Authigenic Ankerite	xxxxxxxxx

Authigenic illite/smec	xxxxxxxxxxx?
Grain contact dissol.	xxxxxxxxxxx......?
Labile grain & ankerite dissolution	xxxxxxxxxx.................?
Authigenic dickite	xxxxxx
Quartz overgrowths	xxxxxxxxxxxxxx

EARLY..LATE
BURIAL HISTORY

FIGURE 2. PARAGENETIC SEQUENCE

6. RESERVOIR QUALITY

Diagenetic processes exert a major influence on reservoir quality, but diagenetic processes are themselves ultimately controlled by original texture (grain size) and composition. This is because the relative importance of major porosity-reducing diagenetic changes such as authigenic clay formation and quartz overgrowth cementation is dependent on the availability of labile grains that are precursors of authigenic clay. Thus, in the cleaner medium and coarse grained sands which contained few labile grains, quartz overgrowths are well developed but good macroporosity still remains. In the finer sands, the abundance of mica and other labiles has resulted in a high content of authigenic clay, limited overgrowth cementation, but widespread grain contact dissolution. These sands are largely microporous and have low permeability. Localized porosity loss also occurs due to the presence of authigenic carbonates.

Within the better quality, medium-very coarse grained reservoir sands, macroporosity is mostly intergranular, although pore sizes have often been considerably reduced by quartz overgrowth cement. The intergranular pores are supplemented by more erratically distributed but larger pores which are interpreted as secondary. The result is that the better sands possess a well-interconnected pore system, although patches of authigenic dickite clay occur in all samples. This clay may provide some potential for fines migration damage to the reservoir, particularly in the medium grained rather than the coarser sands, as pore throats may be small enough to be susceptible to blockage.

Permeability is related mainly to grain size and to the volume of macroporosity. With decreasing grain size, clay content increases, resulting in an increase in the proportion of microporosity and reduced permeability. The relationship between macroporosity as measured from thin-section, and permeability is shown in Figure 3, while the grain size influence on permeability is demonstrated in Figure 4. In this cross-plot, the most coarse grained (3.0mm) sample has been omitted. Its relatively low porosity and permeability are due to the effects of grain contact dissolution, with sutured grain contacts being common, and also to its higher than average content of lithic grains, some of which have compactionally deformed and have been squeezed into adjacent pore spaces. In all cross-plots, permeability values of <0.1mD and >10000mD are recorded as 0.1mD and 10000mD respectively.

FIGURE 3. VISIBLE POROSITY/PERMEABILITY CROSS-PLOT

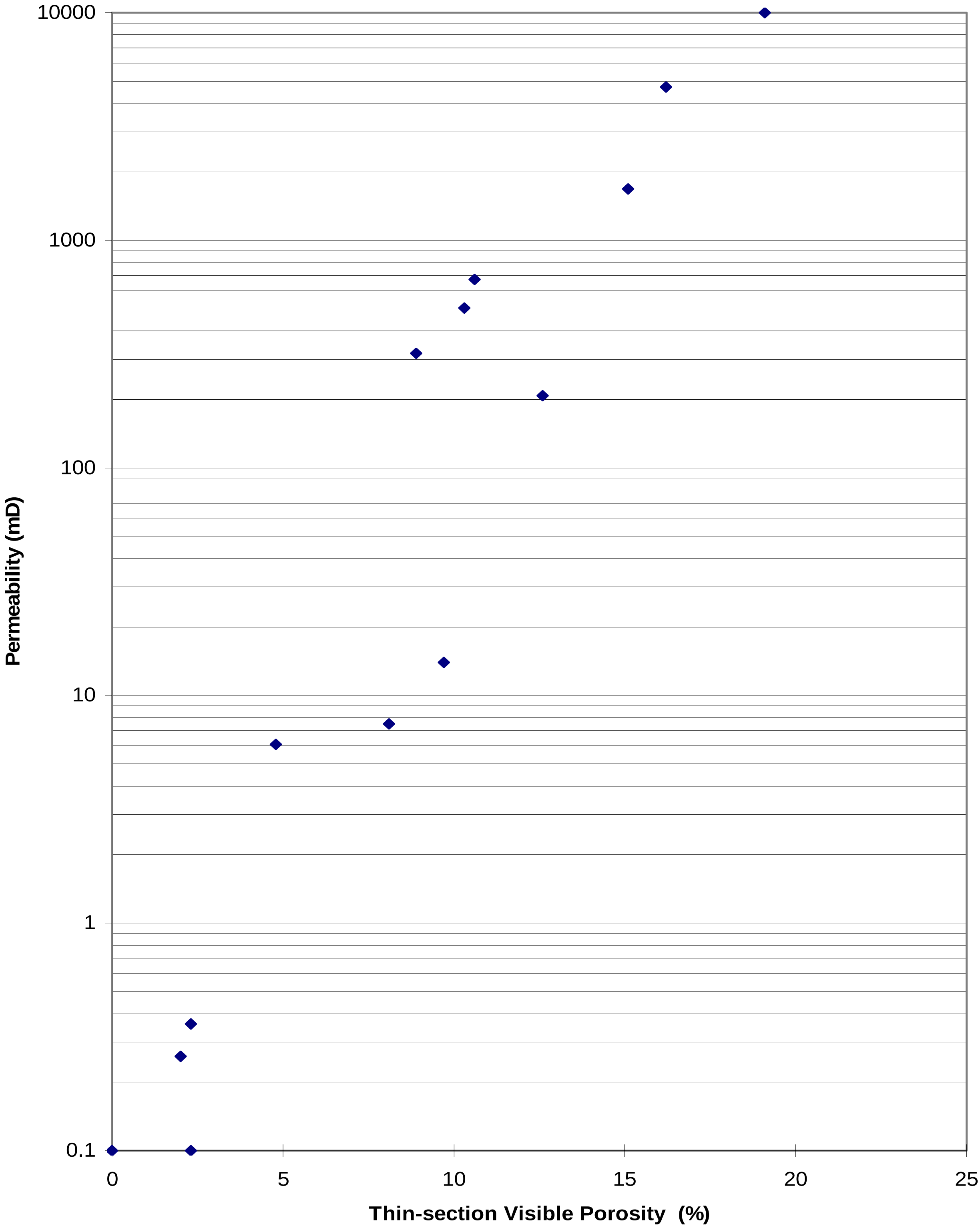

FIGURE 4. AVERAGE GRAIN SIZE/PERMEABILITY CROSS-PLOT

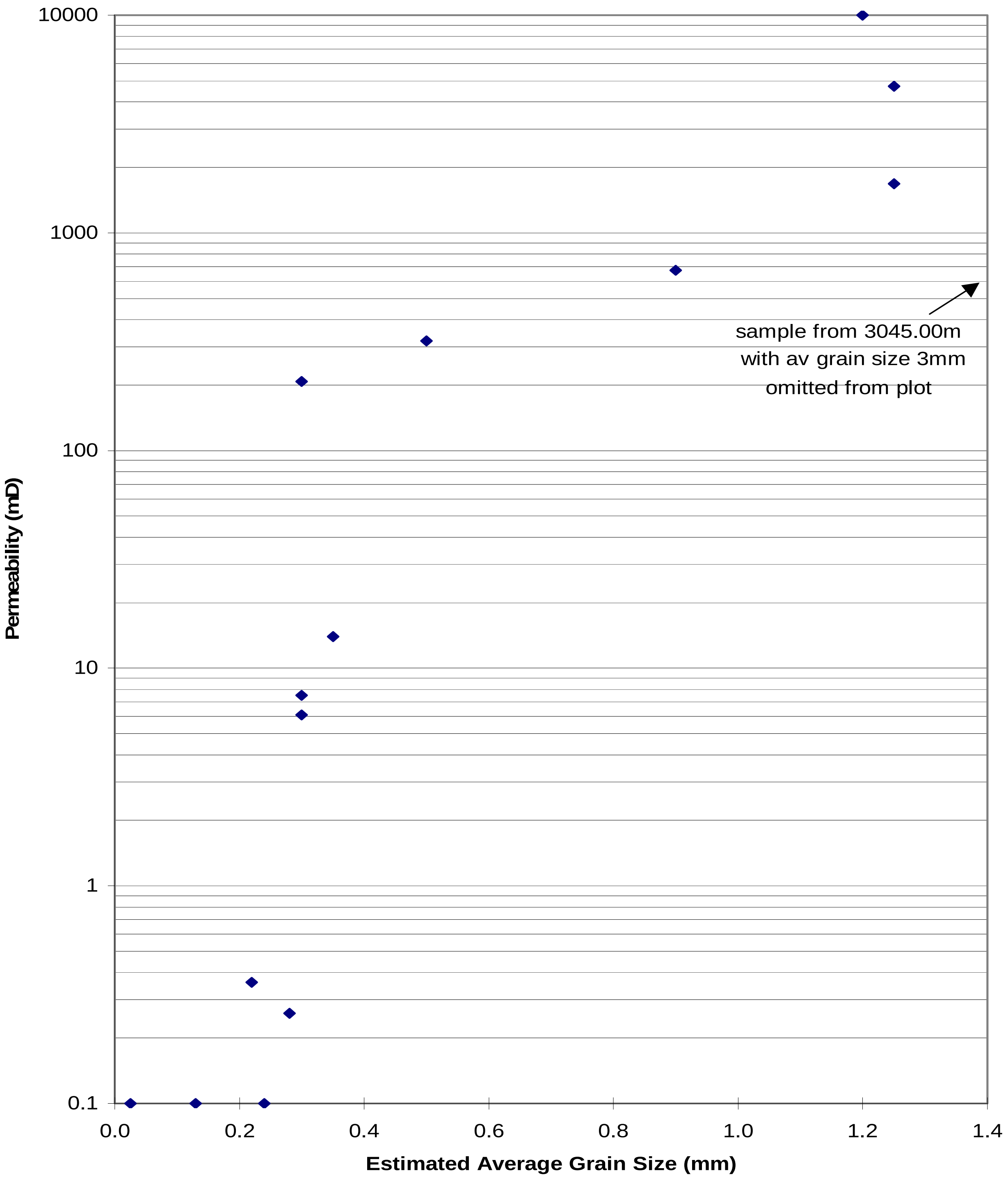

Although reduction in macroporosity and hence permeability may result from a number of different processes including cementation, grain contact dissolution and authigenic clay formation, it is authigenic clay formation which has the most severe adverse effect on reservoir quality in the Yolla-2 samples. The inverse relationship between clay content and permeability is shown in Figure 5.

FIGURE 5. CLAY/PERMEABILITY CROSS-PLOT

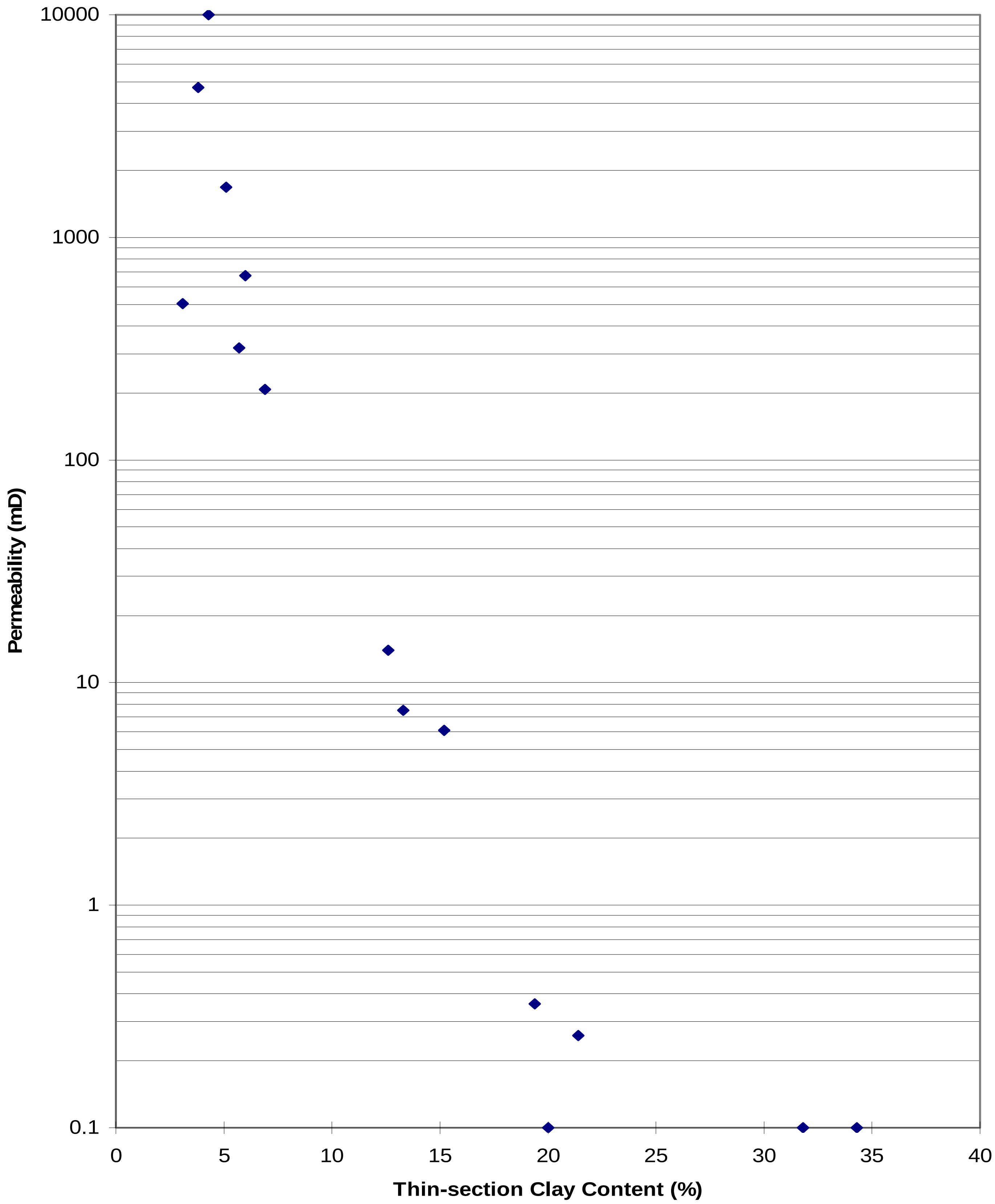

7. CONCLUSIONS

1. Samples from Yolla-2 range in grain size from siltstone to granule conglomerate. All sandstones are quartz-rich sublitharenites and quartzarenites which are almost completely devoid of feldspar but contain minor lithic grains, mainly low-grade metasediments. The samples probably originally contained at least some feldspar and more mica and lithics than are now present but many of these labile grains have since decomposed to authigenic clay.
2. In addition to the formation of authigenic clays which include dickite, kaolinite, illite and illite/smectite, the other main diagenetic changes which have adversely impacted on reservoir quality include quartz overgrowth cementation, grain contact dissolution and carbonate cementation/replacement. These changes have been partly offset in the better reservoir sands by dissolution of labile grains (probably feldspar) and ankerite cement to form minor secondary porosity.
3. The better reservoir sands in Yolla-2 are medium-very coarse grained quartzarenites which, although variably cemented by quartz overgrowths, generally contain little clay and retain a well-interconnected system of intergranular pores supplemented by sporadic secondary pores. With decreasing grain size, clay content and microporosity increase, while macroporosity and hence permeability decrease. The most fine grained samples in the suite are almost totally microporous, with permeability well below 1mD.

8. REFERENCES

Ehrenberg S.N., Aagaard P, Wilson M.J., Fraser A.R., Duthie D.M.L. 1993: Depth-dependent transformation of kaolinite to dickite in sandstones of the Norwegian continental shelf. *Clays Minerals 28*, 325-352

APPENDIX 1. X-RAY TRACES

Key to abbreviations

D	dickite
IM	illite/mica
IS	illite/smectite
K	kaolinite
KCl	potassium chloride
Q	quartz
S	siderite

Yolla-2 3034.05m fine fraction

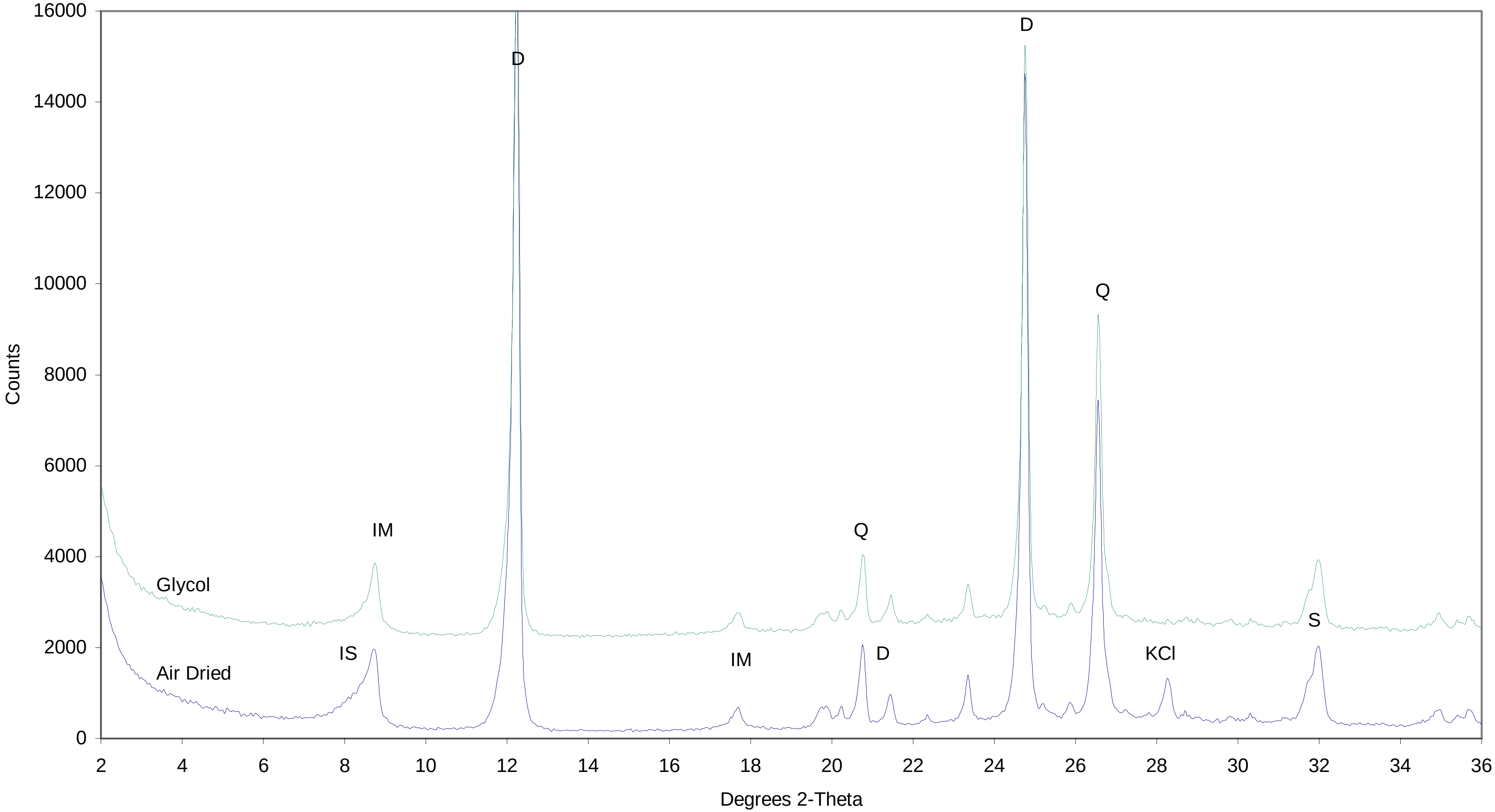

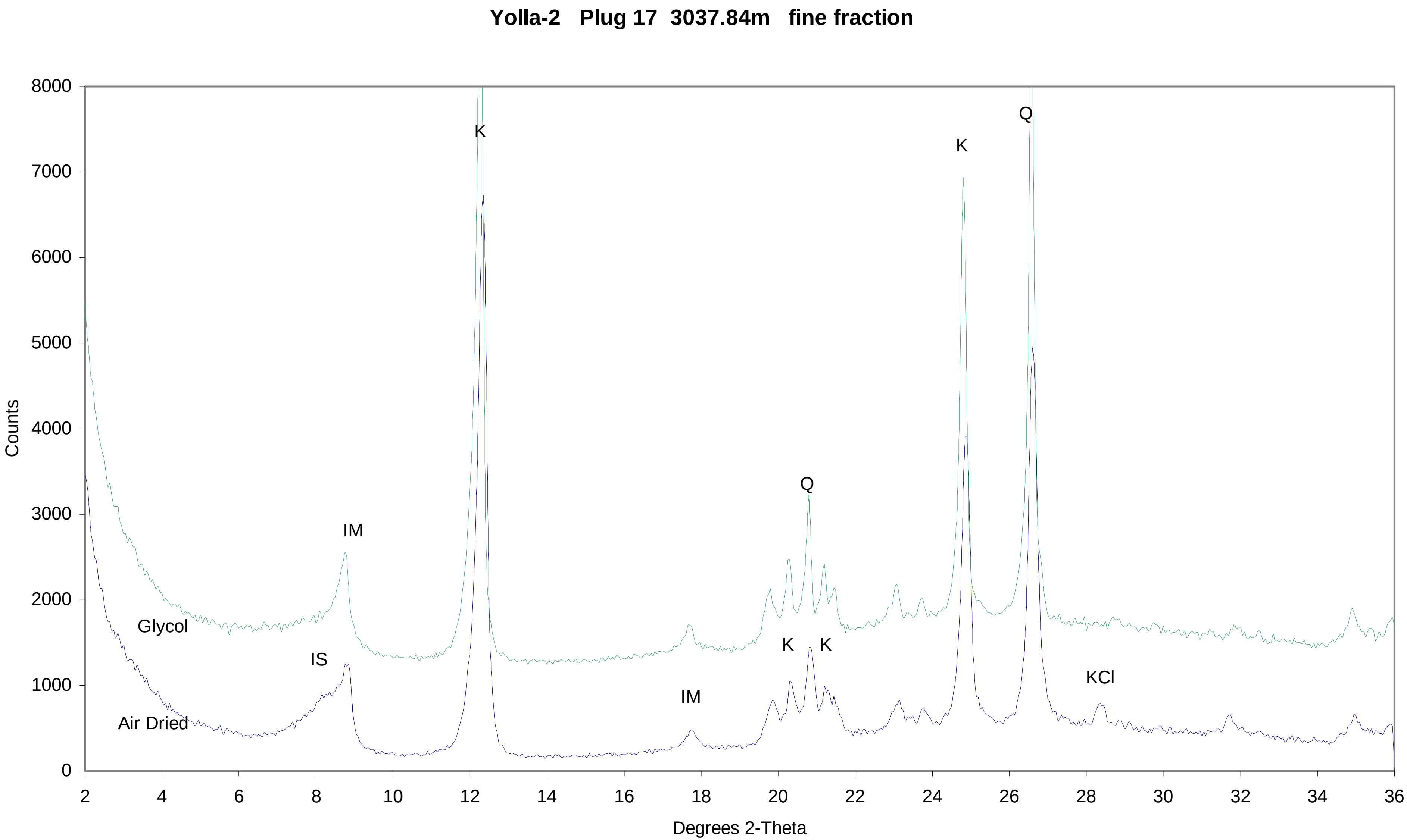
Yolla-2 Plug 17 3037.84m fine fraction
Counts
Degrees 2-Theta
Glycol
Air Dried
IM
IS
K
IM
Q
K
K
K
Q
KCl
0
1000
2000
3000
4000
5000
6000
7000
8000
2
4
6
8
10
12
14
16
18
20
22
24
26
28
30
32
34
36

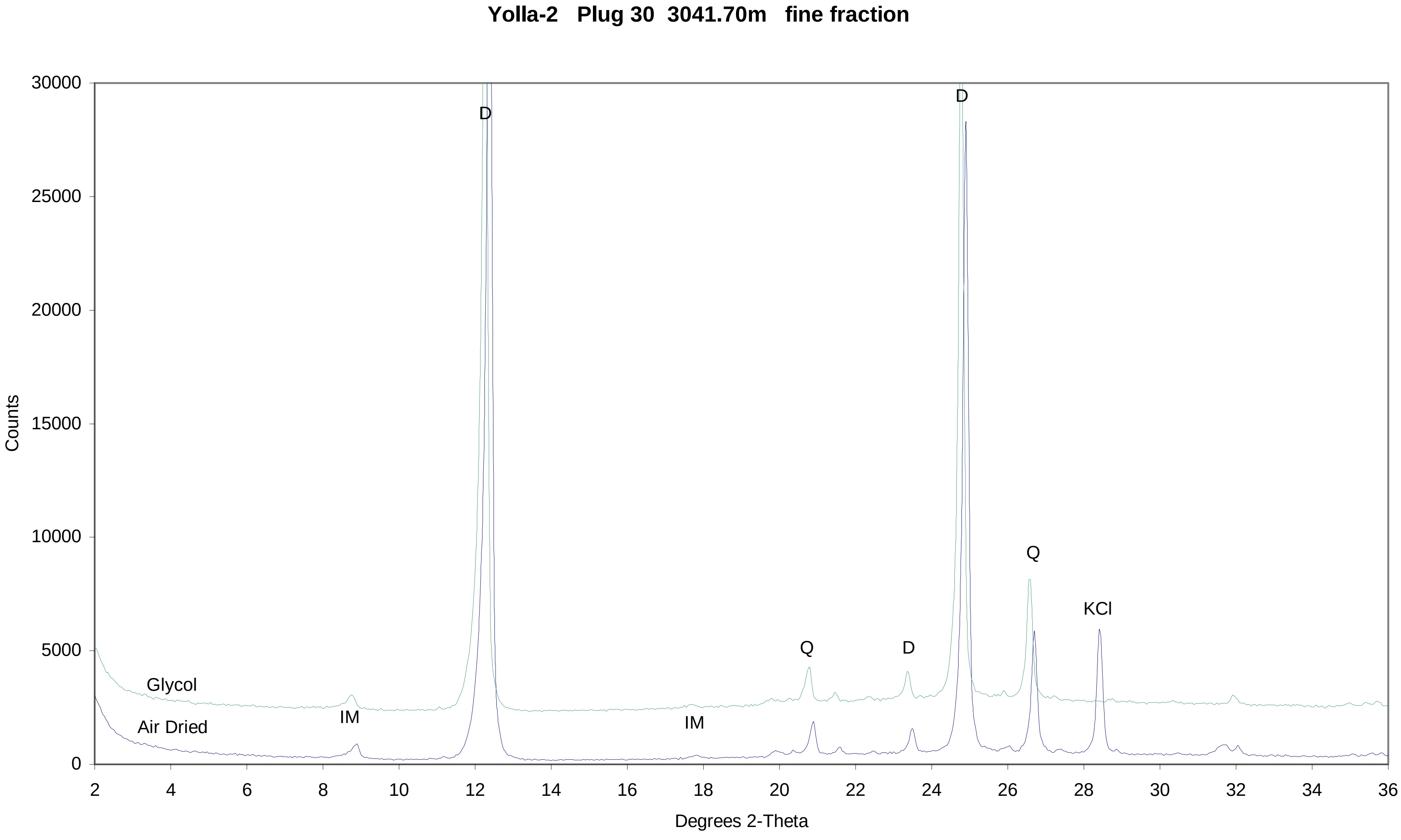

Yolla-2 Plug 30 3041.70m fine fraction
Counts
30000
25000
20000
15000
10000
5000
0
D
D
Q
D
Q
KCl
Glycol
Air Dried
IM
IM
2
4
6
8
10
12
14
16
18
20
22
24
26
28
30
32
34
36
Degrees 2-Theta

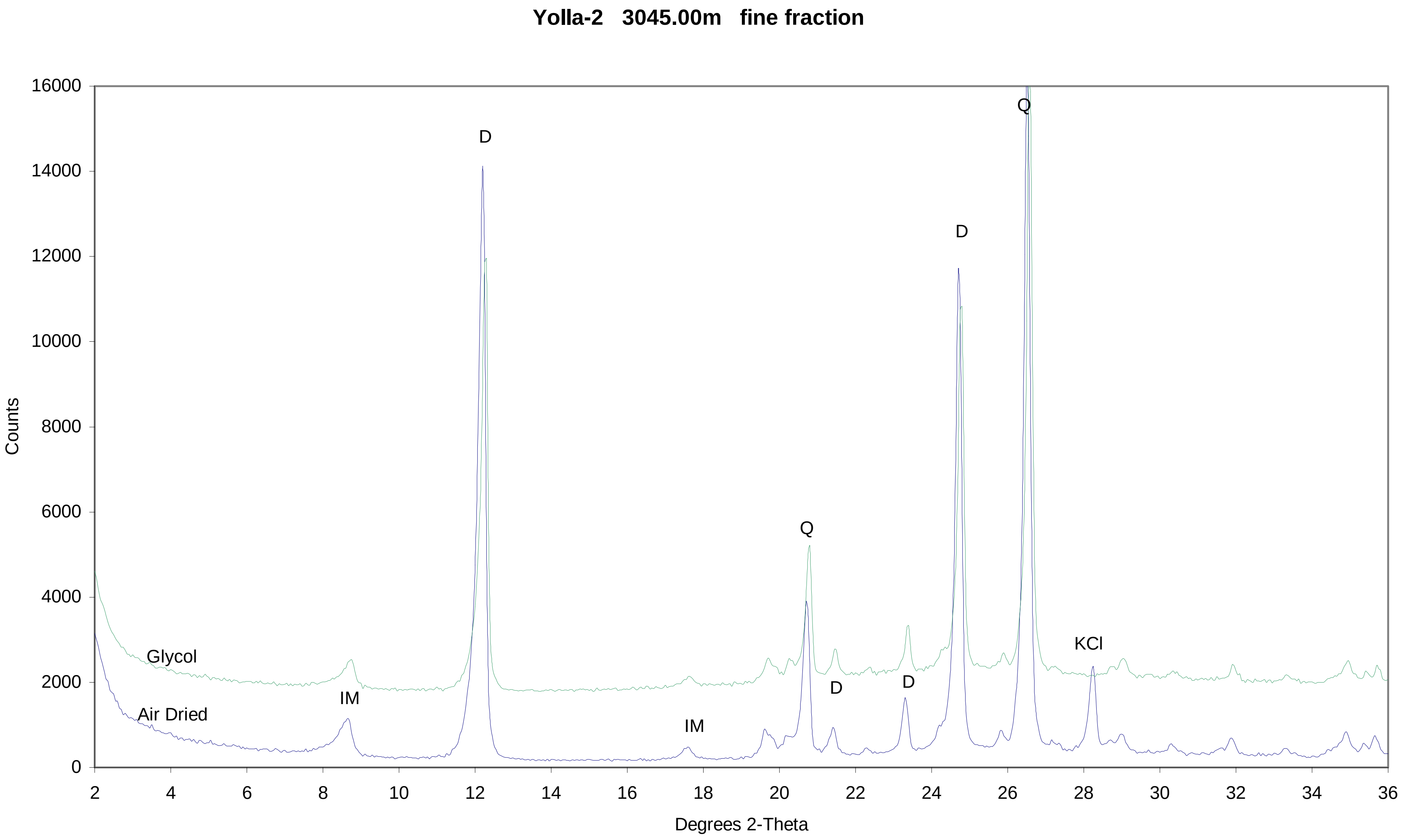
Yolla-2 3045.00m fine fraction
Counts
Degrees 2-Theta
16000
14000
12000
10000
8000
6000
4000
2000
0
2
4
6
8
10
12
14
16
18
20
22
24
26
28
30
32
34
36
Glycol
Air Dried
D
Q
D
Q
IM
IM
D
D
KCl

Yolla-2 Plug 45 3046.14m fine fraction

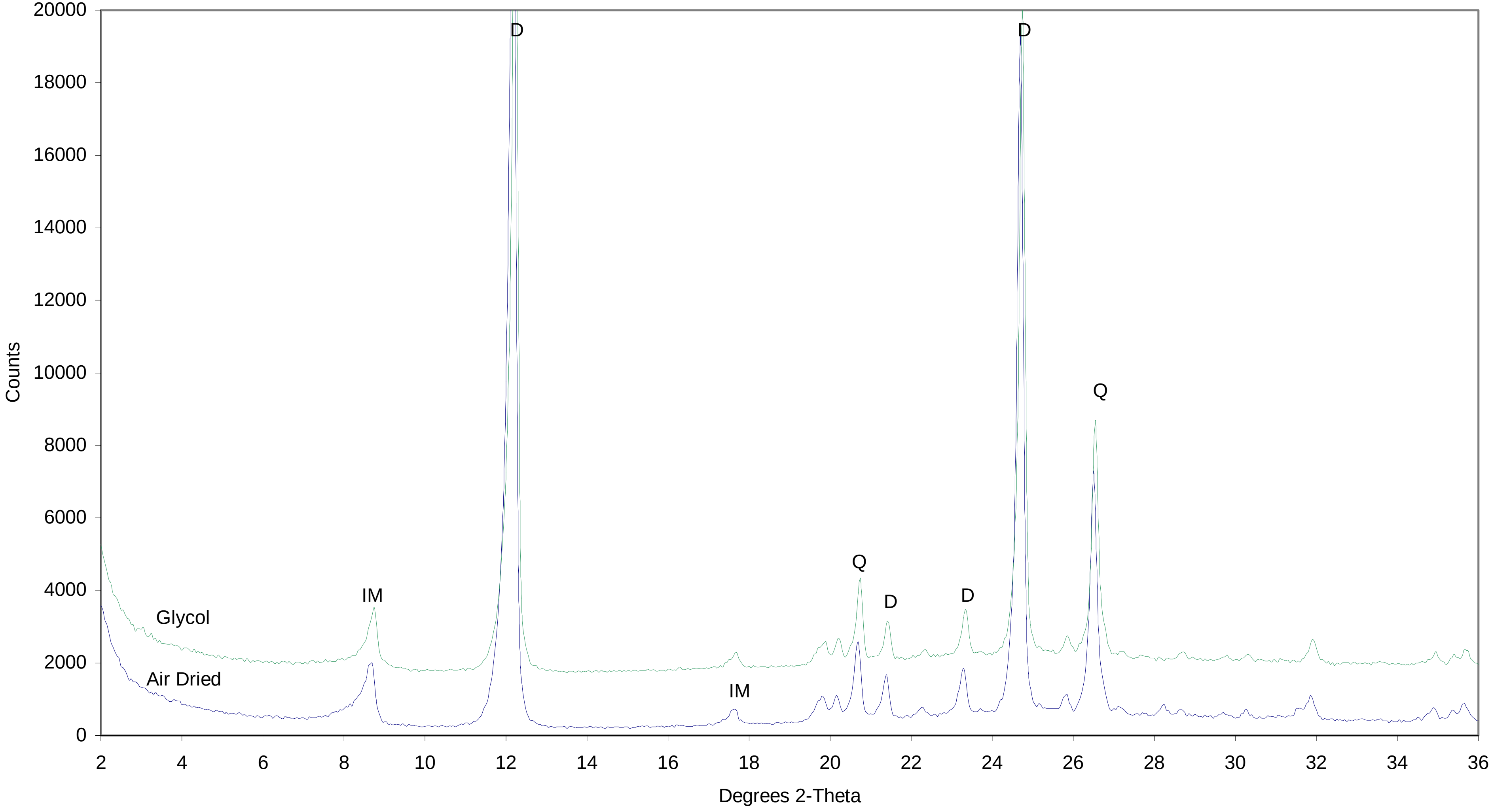

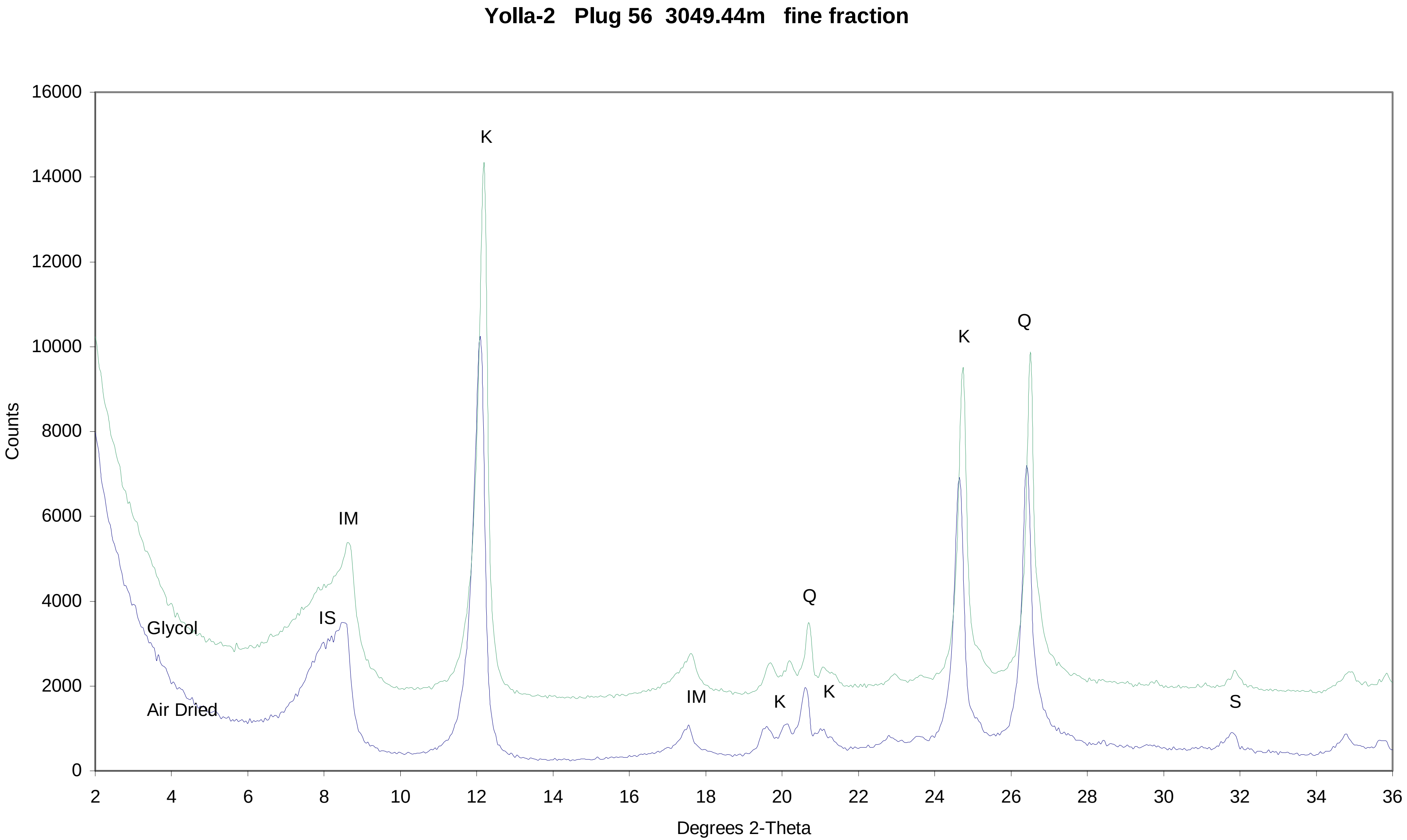
Yolla-2 Plug 56 3049.44m fine fraction
Counts
Degrees 2-Theta
0
2000
4000
6000
8000
10000
12000
14000
16000
2
4
6
8
10
12
14
16
18
20
22
24
26
28
30
32
34
36
Glycol
Air Dried
IM
IS
K
IM
Q
K
K
K
Q
S

APPENDIX 2. PHOTOMICROGRAPHS

PLATE 1 Yolla-2 Plug 1, 3033.03m

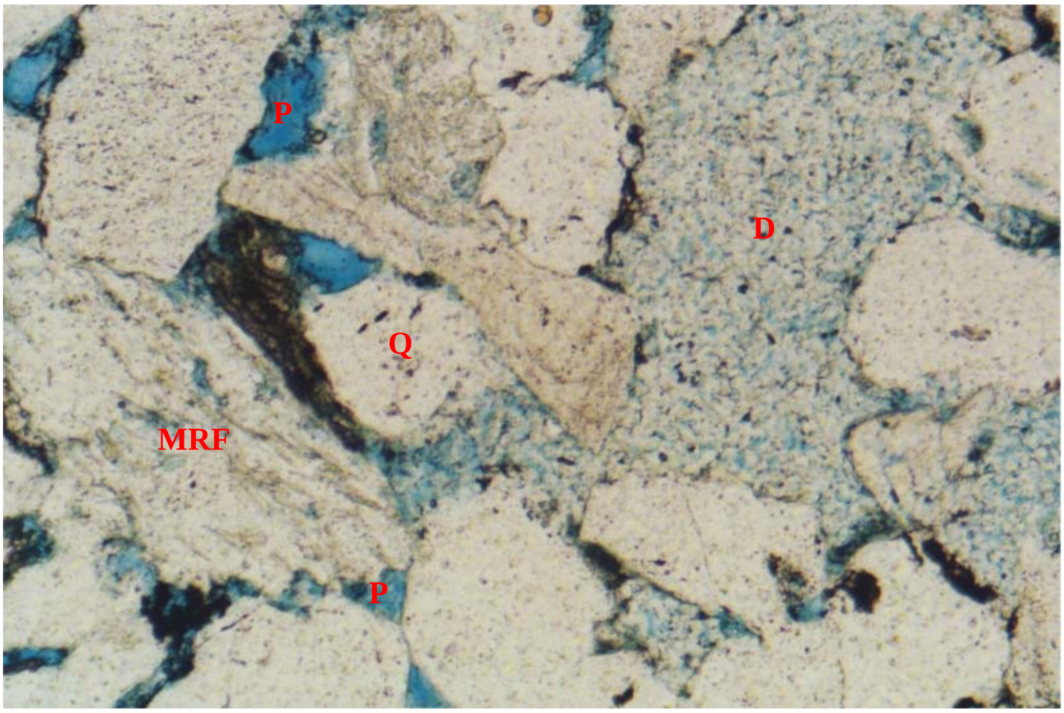

A Plane polarised light

B Crossed polarisers

0.2mm

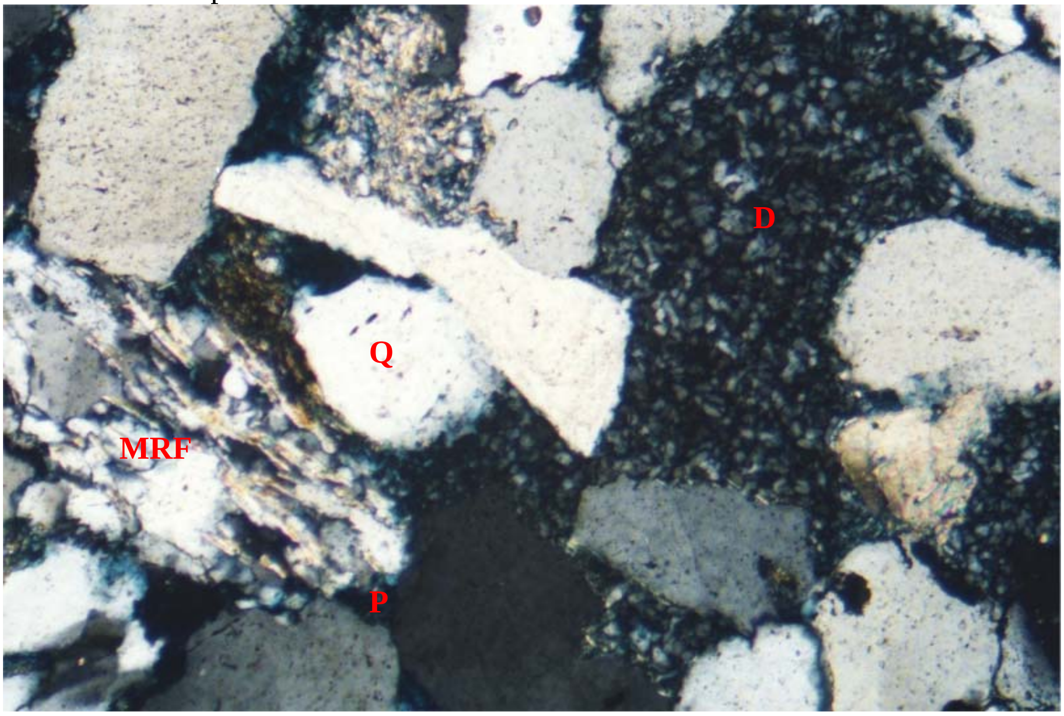

This sandstone contains framework grains of quartz (Q) and metamorphic rock fragments (MRF). Sporadic intergranular pores (P) are present, but much of the pore system is occupied by authigenic dickite (D), with the very large patch of dickite marking the location where a labile grain, probably a feldspar, has totally decomposed.

PLATE 2 Yolla-2 3034.05m

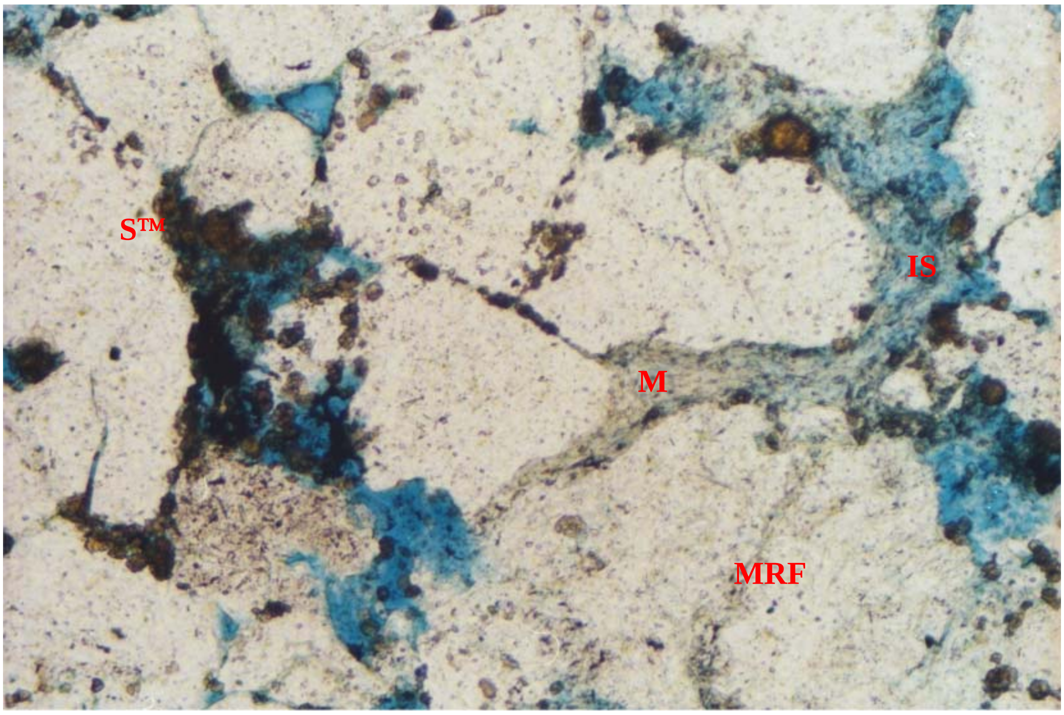

A Plane polarised light

B Crossed polarisers **0.2mm**

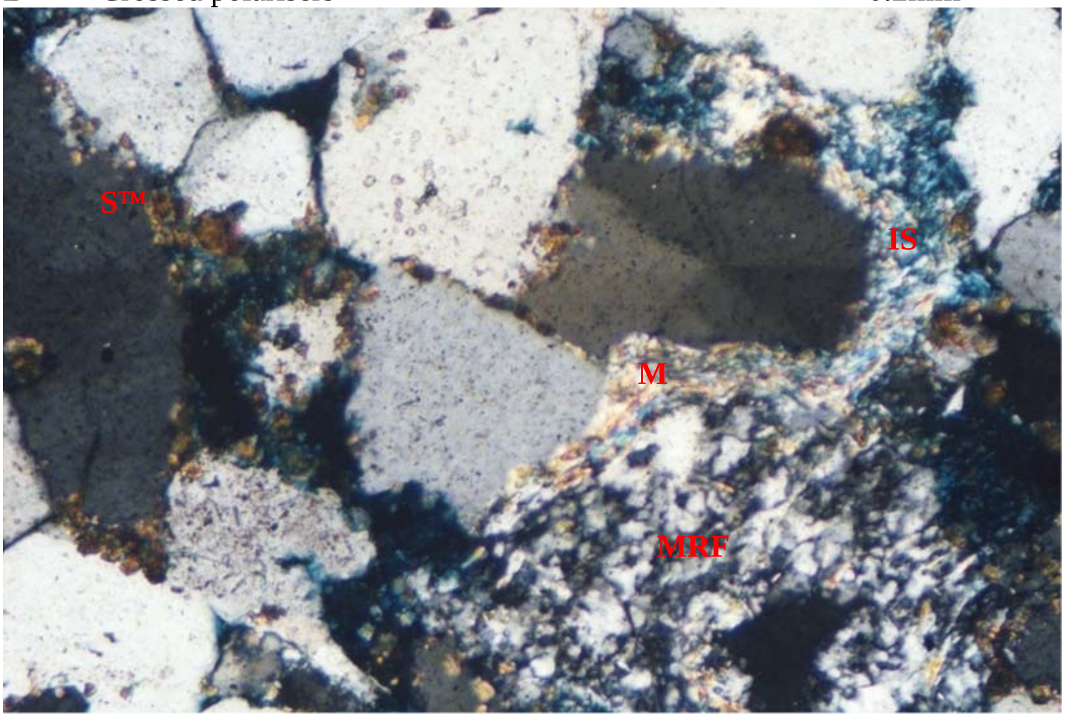

In this sandstone, grains other than quartz include metamorphic rock fragments (MRF) and a deformed grain of mica (M) which is partly decomposed to illite or illite/smectite (IS). Fine grained authigenic siderite (S) lines and partly fills some pores.

PLATE 3 Yolla-2 3034.05m

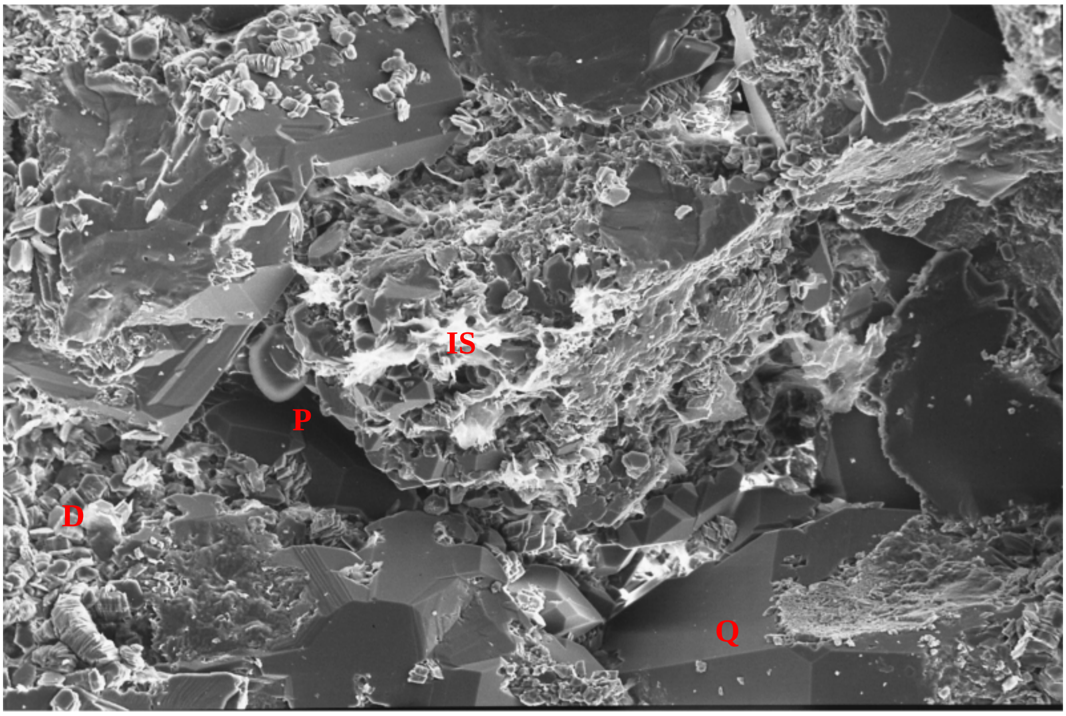

A

100um

This SEM photomicrograph shows quartz grains (Q) on which planar overgrowths have developed. Intergranular pores (P) are sporadic and some pores have been filled by authigenic dickite (D), while illite/smectite (IS) can be seen coating a few grain surfaces.

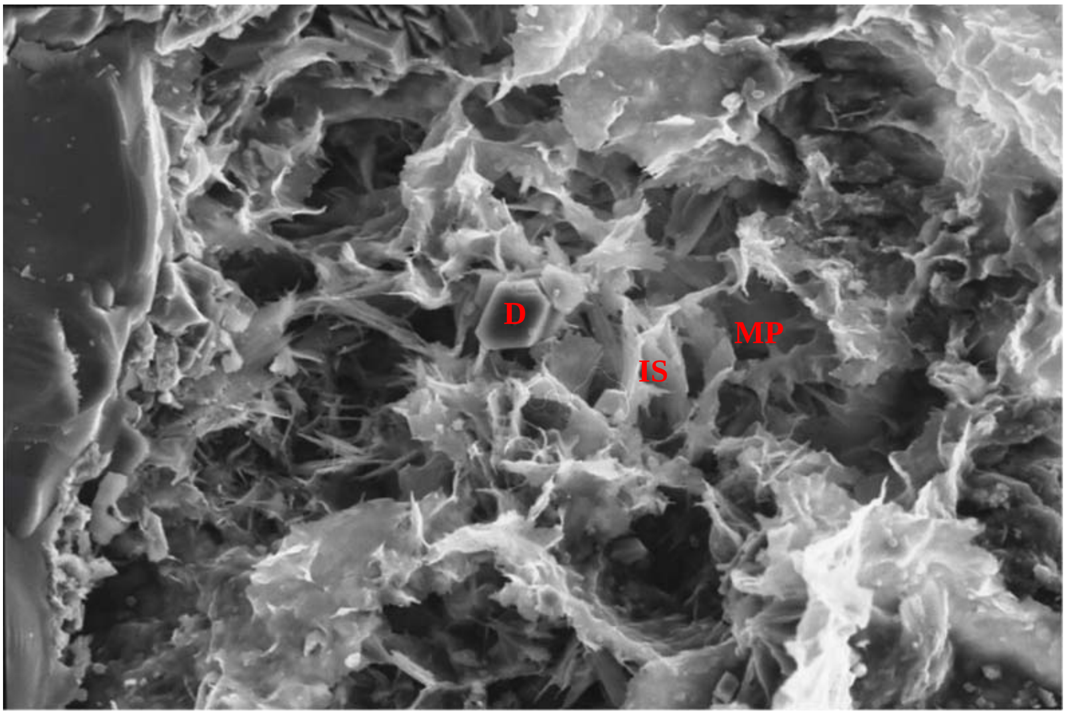

B

10um

Detail of a pore filled by a network of crenulated, platy illite/smectite (IS) crystals with large volumes of interstitial microporosity (MP). An isolated dickite (D) crystal is also marked.

PLATE 4 Yolla-2 3034.05m

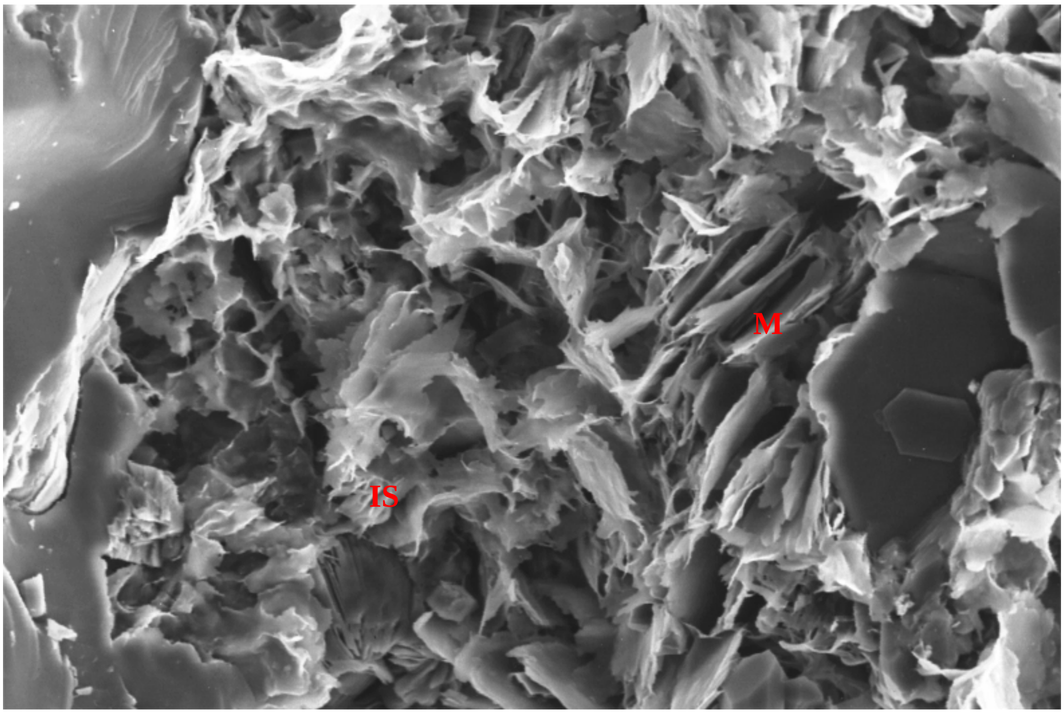

A

10um

This is an example of a mica grain which has almost totally decomposed to authigenic illite/smectite (IS), now occupying all the adjacent pore space. Only in a few places are the mica crystals (M) still recognisable.

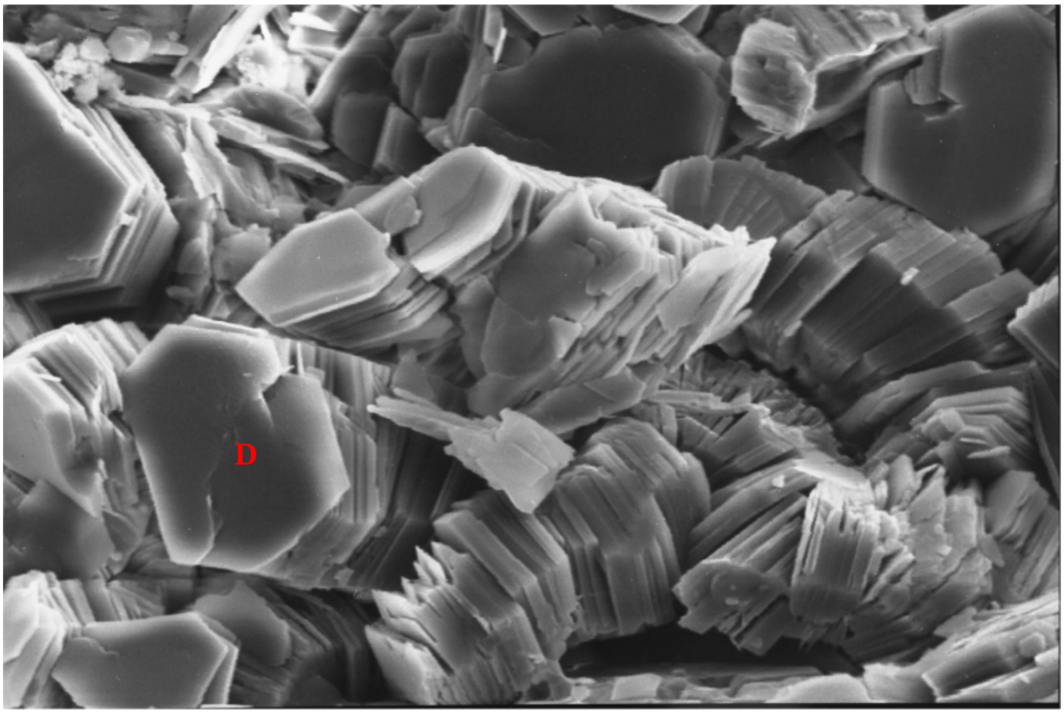

B

10um

Detail of typical pore-filling authigenic dickite (D) showing the stacked, platy, pseudohexagonal crystals

PLATE 5 Yolla-2 Plug 14, 3036.95m

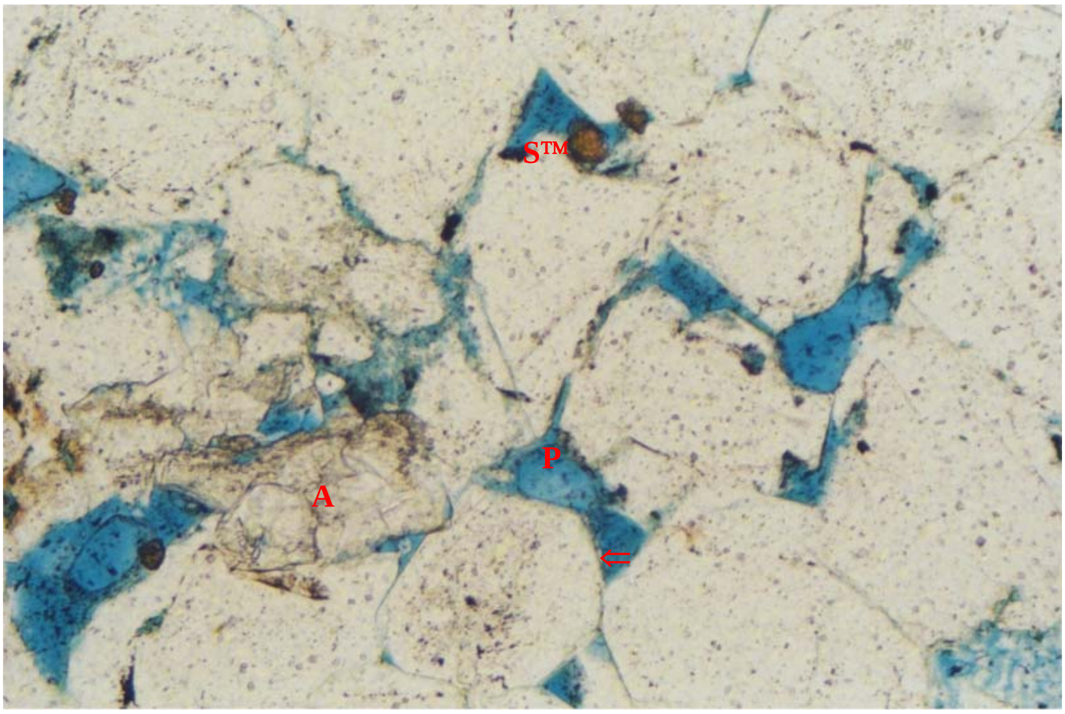

A Plane polarised light

B Crossed polarisers

0.2mm

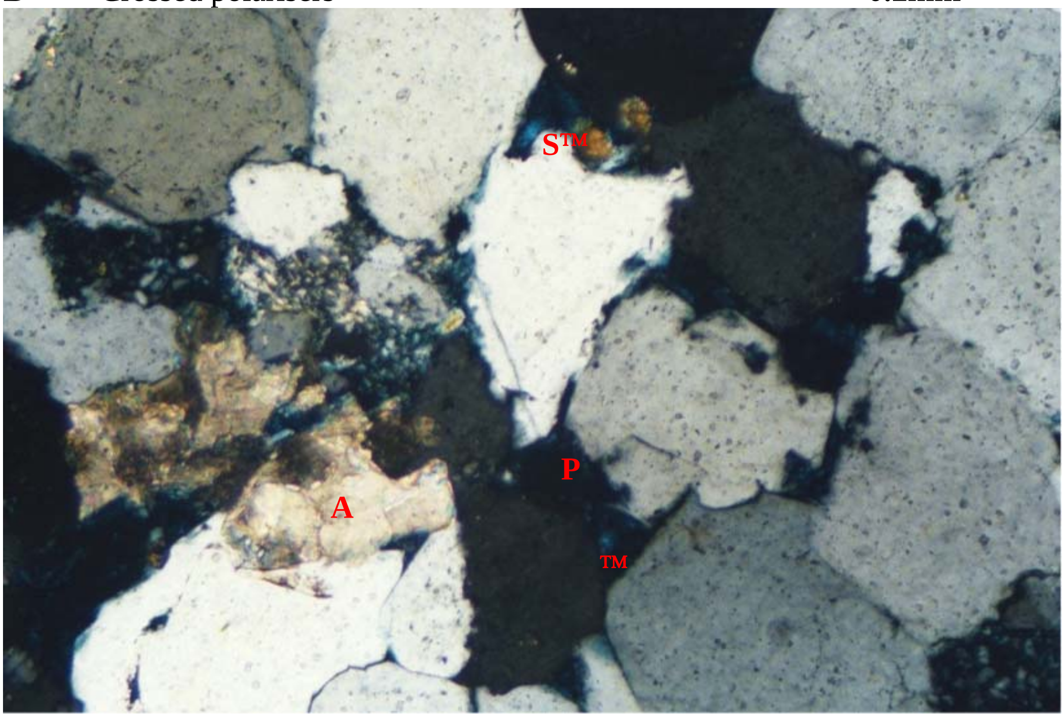

This sandstone has been well cemented by quartz overgrowths which can be seen as planar crystal faces (arrow) bordering many of the intergranular pores (P). Also visible are corroded crystals of ankerite (A) and several small siderite (S) crystals.

PLATE 6 Yolla-2 Plug 14, 3036.95m

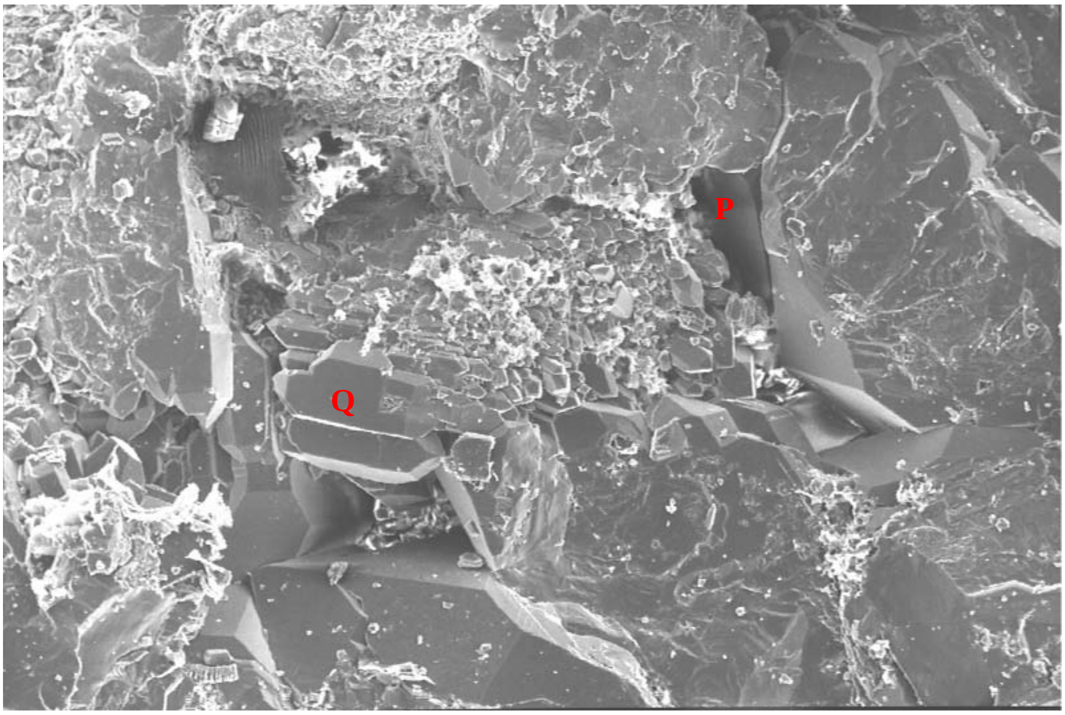

A

100um

The relatively advanced quartz overgrowth cementation can be seen in this SEM photomicrograph, with almost all quartz grains (Q) exhibiting planar crystal faces. Despite the extent of cementation, numerous intergranular pores (P) are present.

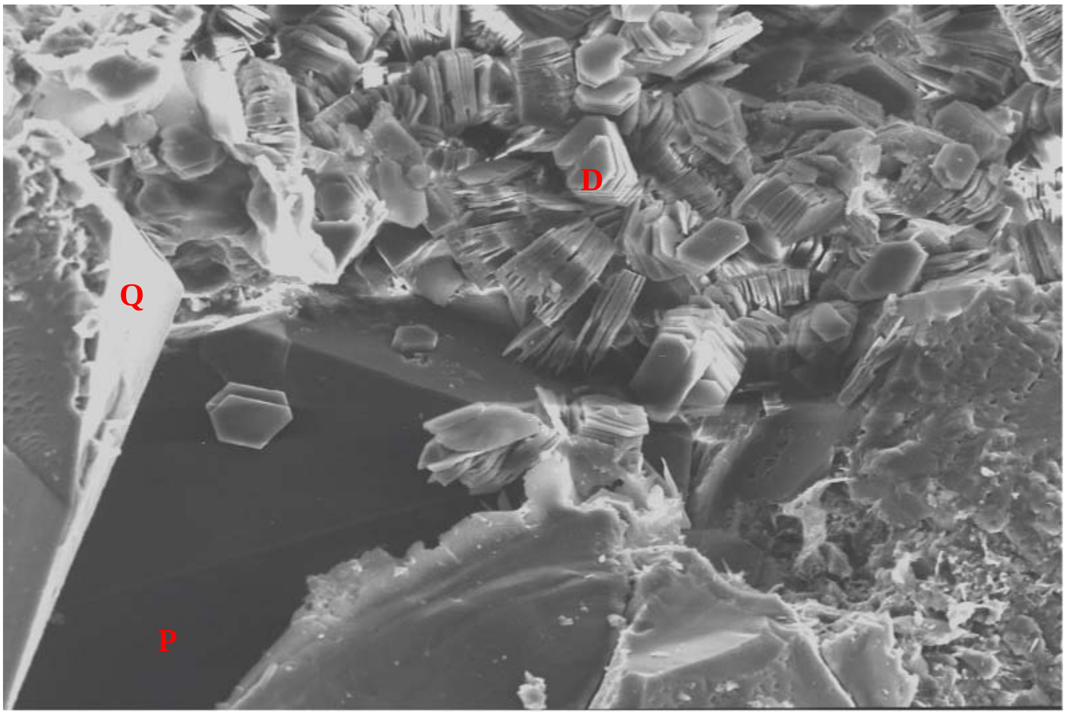

B

10um

Detail of a pore (P) partly filled by authigenic kaolin clay which is probably dickite (D). Quartz (Q) overgrowth crystal faces border the pore.

PLATE 7 Yolla-2 Plug 27, 3040.81m

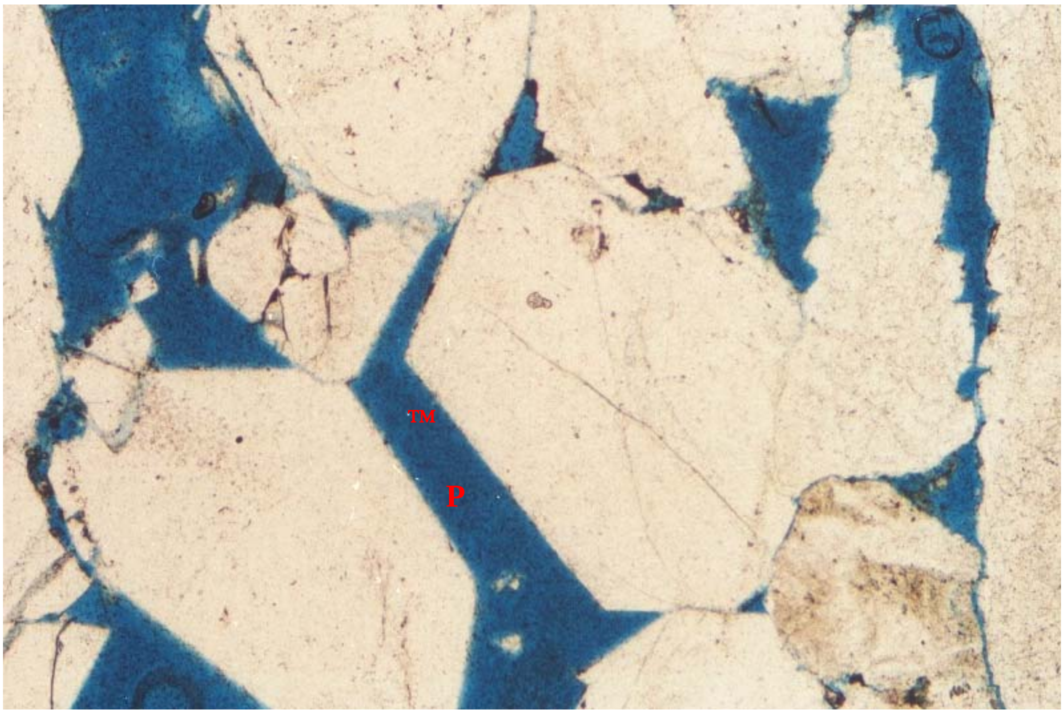

A Plane polarised light
B Crossed polarisers

0.5mm

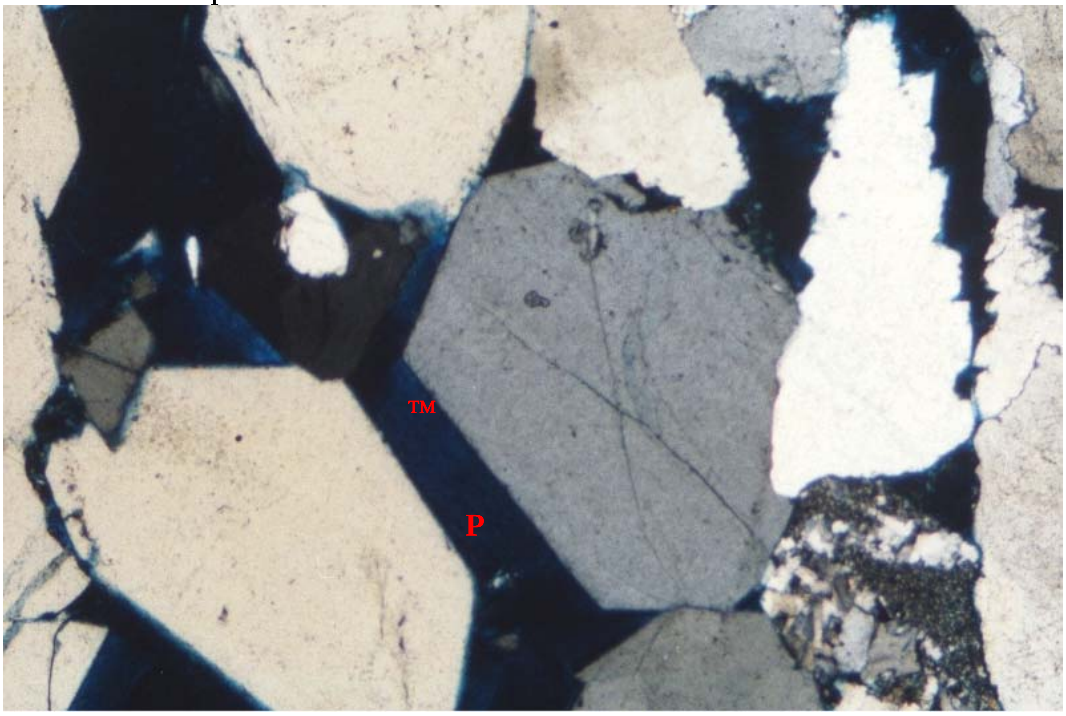

In this very coarse grained highly permeable sandstone, excellent intergranular porosity (P) is retained despite the presence of quartz overgrowths, the planar faces of which border most pores (arrow).

PLATE 8 **Yolla-2 Plug 27, 3040.81m**

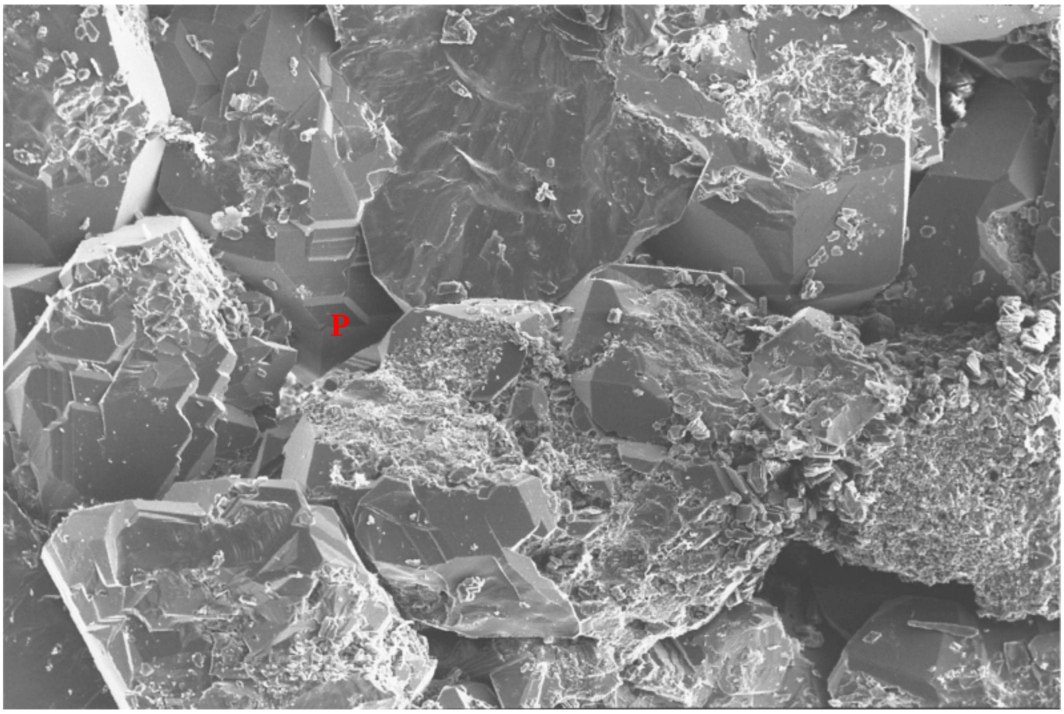

A

100um

SEM photomicrograph showing a sandstone with abundant intergranular porosity (P) despite widespread quartz overgrowth cementation.

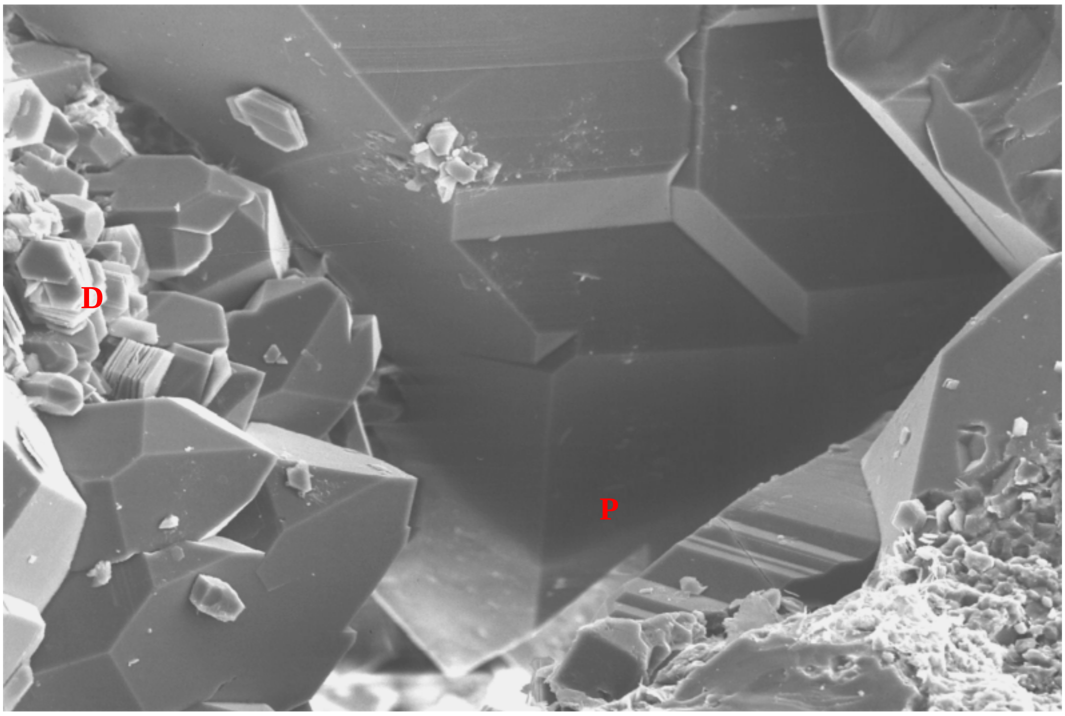

B

10um

Detail of a pore (P) bounded by planar quartz overgrowth crystal faces. The smaller dog-toothed quartz overgrowth crystals visible on the left have probably developed on a composite quartz grain. Rare crystals of dickite (D) can be seen amongst the overgrowth crystals.

.